Eclética Química Journal

Original article
iq.unesp.br/ecletica

| Vol. 45 | n. 3 | 2020 |

Major and minor head losses in a hydraulic flow circuit: experimental measurements and a Moody's diagram application

Aline Amaral Madeira[1+]
Pontifical Catholic University of Minas Gerais (PUC-MG), 500 Dom José Gaspar Av, Belo Horizonte, Minas Gerais, Brazil

[+]Corresponding author: Aline Amaral Madeira, Phone: +55 31 991807451, Email address: madeira.alineamaral@gmail.com

ARTICLE INFO

Article history:
Received: June 13, 2019
Accepted: January 31, 2020
Published: July 1, 2020

Keywords:
1. head loss
2. hydraulic circuit
3. head loss coefficient
4. friction factor
5. Moody's diagram

ABSTRACT: Domestic and industrial hydraulic drainage networks have gradually become more complicated because of the cities' rapid expansion. In surcharged hydraulic systems, the head losses may become rather significant, and should not be neglected because could result in several problems. This work presents an investigation about major and minor head losses in a hydraulic flow circuit, simulating the water transport in a drainage network at room temperature (298.15 K) under atmospheric pressure (101,325 Pa). The losses produced by the fluid viscous effect through the one used cast-iron rectilinear pipe (RP-11) and the localized losses generated by two flow appurtenances, one fully open ball valve (BV-1) and one module of forty-four 90º elbows (90E-8) were experimentally measured. Experimental data generated head-loss curves and their well fitted to potential regressions, displaying correlation coefficients (R^2) of 0.9792, 0.9924, and 0.9820 for BV-1, 90E-8, and RP-11, respectively. Head loss experimental equations and local loss coefficients through BV-1 and 90E-8 were determined successfully. The Moody's diagram application proved to be a quite appropriate tool for an approximate estimation of Darcy-Weisbach friction factor. A good approximation between friction factor values obtained via experimental measurements and the Moody's diagram was observed with mean absolute deviate of 0.0136.

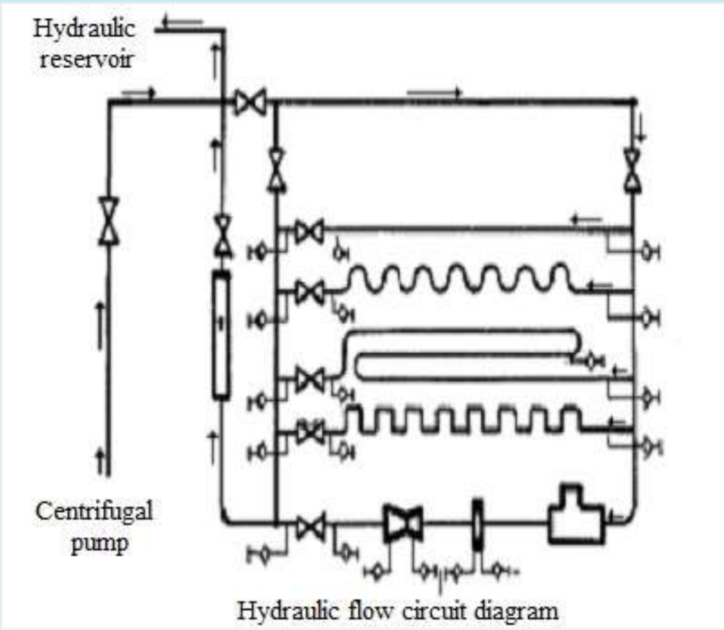

1. Introduction

Pipeline systems range from the quite simple ones to large and quite complex ones. They may be as uncomplicated as a single pipe conveying water from one reservoir to another or they may be as elaborate as an interconnected set of water distribution networks for a major metropolitan area[1]. The hydraulic drainage domestic and industrial networks have gradually become more complicated and diverse because of the cities' rapid urbanization and expansion. In surcharged hydraulic systems, the head losses may become rather significant, and should not be neglected because could result in several problems, such as inappropriate drainage pipes, insufficient carrying capacities, blowout of manhole covers and the occurrence of floods, for example[2].

Groundwater flow and solute transport in fractured rock is of great interest in nuclear waste disposal, contaminant control, and oil recovery. The friction factor is an important parameter in identifying the characteristics of flow and solute hydraulic transport. During the last several decades, several theoretical and experimental researches have been conducted to investigate the

CC BY

relationship between the friction factor and the Reynolds number. Colebrook[3] realized experiments on several types of pipes and the results were correlated to the well-known Colebrook equation. Later, Moody[4] presented Colebrook's results in a graphical format, which is called the Moody diagram[5,6]. Moody's diagram represents the plots of the Colebrook equation over a very wide range of the Reynolds number (Re from 2320 to 10^8) and relative roughness values (ε/D from 0 to 0.05)[7].

According to LaViolette[8], Moody's chart provides an easy and accurate way of solving hydraulic flow and dimensioning problems, making it an extremely useful tool and unmistakable simplicity adopted by engineers to understand the behavior of viscous flows and evaluate the loss of energy due to viscous friction. The diagram is available in most fluid mechanics textbooks and is widely used to estimate the effects of pipe roughness on pipe friction as a function of Reynolds number[9].

Water flows are turbulent flows and the hydraulic calculations in water networks still have certain indetermination, particularly due to the velocity of the flow is rather small[10,11]. In a typical system with long pipes, there are the major head losses, related to friction between the flowing fluid and pipeline systems, and minor losses. Although this is generally true, in some cases the minor losses may be greater than the major losses. This is the case, for example, in systems with several turns and valves in a short distance. Several design parameters of pipelines used in domestic and industrial networks could be calculated and optimized if all major and minor head losses of such pipelines are well estimated by hydraulic calculations[10].

Local head losses are any energy loss caused by some localized disruption of the flow due to the presence of various flow appurtenances, such as valves, bends, elbows, inlets, exits, enlargement, and contractions in addition to the pipes. These components interrupt the smooth flow of the fluid and cause additional losses because of the flow separation and mixing they induce. If a loss is sufficiently small in comparison with other energy losses and with pipe friction, it may be regarded as a minor loss. Often minor losses are neglected, or they are known to be quite small, as happen in very long pipes. However, some local losses can be so large or significant that they will never be termed a minor loss. Normally, theory alone is unable to quantify the magnitudes of the energy losses caused by these devices, so the representation of these losses depends heavily upon experimental data[1].

In this context, the present work ambulates to delineate a new investigation about major and minor head losses in a hydraulic flow circuit used for water fluid transport at room temperature (298.15 K) under atmospheric pressure (101,325 Pa). It strives to measure the head losses produced by the fluid viscous effect through the rectilinear pipe of used cast-iron and the localized losses generated by one fully open ball valve and one module composed by forty-four 90º elbows. Focusing on the experimental determinations of the local head loss coefficients and of the Darcy-Weisbach friction factor, besides providing subsidies for an application of Moody's diagram to the behavior of the hydraulic flow of the mentioned circuit. In addition, this work aims at presenting an application approach of theoretical concepts associated with fluid mechanics' and hydraulic's intrinsic fundamentals in the understanding of how head loss measurements can to aid to develop improvements and solutions in the scope of surcharged hydraulic systems of drainage networks.

2. Experimental

Experimental measurements of major and minor head losses were realized in hydraulic flow circuit at room temperature (298.15 K) under atmospheric pressure (101,325 Pa) using water as fluid flow, based on the methodology proposed by Buonicontro[12]. The circuit was composed by a test bench with a pressure-loss module (Didacta, model SUE 14D SU) containing one ball valve, one module of forty-four 90º elbows, and one rectilinear pipe of used cast-iron (Figs. 1 and 2).

In the first test, measures of variability in volumetric flow rate (m^3 h^{-1}) and the corresponding pressure loss (mmHg) were experimentally collected through of the fully open ball valve (BV-1) (Fig. 3). For that, only the connections between the BV-1 and differential pressure gauge (DPG-19) (Fig. 4) were kept open, so that, the components: male-female valve (MFV-2); diaphragm valves (DV-3 and DV-14); drawer valves (DV-4 and DV-16); butterfly valve (BV-5) were closed and the components: ball valve (BV-1); drawer valves (DV-15, DV-17, and

Eclética Química Journal, vol. 45, n. 3, 2020, 47-56
ISSN: 1678-4618
DOI: 10.26850/1678-4618eqj.v45.3.2020.p47-56

DV-18) were opened. Then, the hydraulic circuit centrifugal pump was started and DV-14 was slowly open for flow and pressure variation readings, using rotameter (R-13) (Fig. 5) and differential pressure gauge (DPG-19), respectively. Readings were realized in hydraulic flow range of 3.0 to 9.0 $m^3 h^{-1}$. Figure 6 presents the identification of all hydraulic circuit components and Tab. 1 exhibits the ball valve's experimentally measured data.

Figure 1. Hydraulic flow circuit.

Figure 2. Hydraulic flow circuit control panel.

Figure 3. Ball valve.

Figure 4. Differential pressure gauge coupled to the circuit.

Figure 5. Rotameter coupled to the circuit.

Eclética Química Journal, vol. 45, n. 3, 2020, 47-56
ISSN: 1678-4618
DOI: 10.26850/1678-4618eqj.v45.3.2020.p47-56

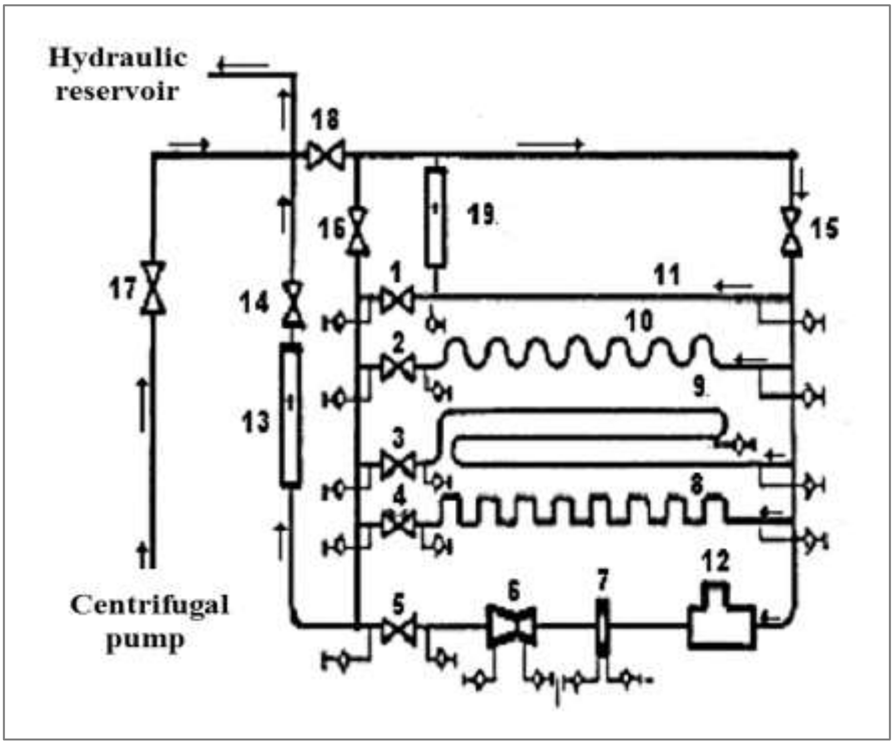

Figure 6. Hydraulic flow circuit identification diagram (BV-1: ball valve; MFV-2: male-female valve; DV-3 and DV-14: diaphragm valves; DV-4, DV-15, DV-16, DV-17, and DV-18: drawer valves; BV-5: butterfly valve; VM-6: venturi meter; OPM-7: orifice plate meter; 90E-8: module of forty-four 90º elbows; RP90C-9: rectilinear pipe with 90º curve; 90C-10: 90º curves module; RP-11: rectilinear pipe; H-12: hydrometer; R-13: rotameter; DPG-19: differential pressure gauge).

Table 1. Ball valve experimental data.

Flow / $m^3\ h^{-1}$	Flow / $m^3\ s^{-1}$	Head Loss / mmHg	Head Loss / mH_2O	Experimental Constant / $mH_2O\ (m^3\ s^{-1})^{-2}$	Mean Experimental Constant / $mH_2O\ (m^3\ s^{-1})^{-2}$	Statistical Parameters (Values in Module)		
						Absolute Deviate	Relative Deviate	Percentage Deviation/%
3.0	8.3E-04	1.0	1.4E-02	2.0E+04	3.3E+04	1.3E+04	4.1E-01	40.8
4.0	1.1E-03	3.0	4.1E-02	3.3E+04		2.3E+01	7.0E-04	0.1
5.0	1.4E-03	5.0	6.8E-02	3.5E+04		2.2E+03	6.6E-02	6.6
6.0	1.7E-03	7.0	9.5E-02	3.4E+04		1.2E+03	3.6E-02	3.6
7.0	1.9E-03	10.0	1.4E-01	3.6E+04		2.9E+03	8.8E-02	8.8
8.0	2.2E-03	14.0	1.9E-01	3.9E+04		5.5E+03	1.7E-01	16.6

In the second test, measures of variability in volumetric flow rate ($m^3\ h^{-1}$) and the corresponding pressure loss (mmHg) were gathered through of the module of forty-four 90º elbows (90E-8). For this, the connection valves of flow input of the first elbow and flow output of the last elbow with the DPG-19 were opened, so that, the components BV-1, MFV-2, DV-3, DV-14, BV-5, and DV-16 were closed and the components DV-4, DV-15, DV-17, and DV-18 were opened. Next, the centrifugal pump was started, and DV-14 was slowly open for flow and pressure variation readings, using R-13 and DPG-19, respectively. Readings were realized in hydraulic flow range of 3.0 to 6.0 $m^3\ h^{-1}$. Table 2 exhibits the 90º elbows module obtained data.

Finally, in the third test, measures of variability in volumetric flow rate ($m^3\ h^{-1}$) and the pressure loss (mmHg) were collected through of the rectilinear pipe of used cast-iron (RP-11) of length of 2.2 m and diameter of 0.0365 m. For that, the connections between the RP-11 and DPG-19 were kept open, so that, the components MFV-2, DV-3, DV-14, DV-4, DV-16, and BV-5 were closed and the components BV-1, DV-15, DV-17, and DV-18 were opened. Then, the

Eclética Química Journal, vol. 45, n. 3, 2020, 47-56
ISSN: 1678-4618
DOI: 10.26850/1678-4618eqj.v45.3.2020.p47-56

centrifugal pump was started, and DV-14 was slowly open for flow and pressure variation readings, using R-13 and DPG-19, respectively. Readings were realized in hydraulic flow range of 3.0 to 9.0 $m^3 h^{-1}$. Table 3 shows the rectilinear pipe obtained data.

Table 2. 90º elbows module experimental data.

Flow / $m^3 h^{-1}$	Flow / $m^3 s^{-1}$	Total Head Loss / mmHg	Unit Head Loss / mmHg	Unit Head Loss / mH_2O	Experimental Constant / $mH_2O (m^3 s^{-1})^{-2}$	Mean Experimental Constant / $mH_2O (m^3 s^{-1})^{-2}$	Statistical Parameters (Values in Module)		
							Absolute Deviate	Relative Deviate	Percentage Deviation/%
3.0	8.3E-04	110.0	2.5E+00	3.4E-02	4.9E+04	5.4E+04	4.6E+03	9.1E-01	91.4
3.5	9.7E-04	144.0	3.3E+00	4.5E-02	4.7E+04		6.5E+03	8.8E-01	87.9
4.0	1.1E-03	206.0	4.7E+00	6.4E-02	5.2E+04		2.0E+03	9.6E-01	96.3
4.5	1.3E-03	295.0	6.7E+00	9.1E-02	5.8E+04		4.8E+03	1.1E+00	109.0
5.0	1.4E-03	358.0	8.1E+00	1.1E-01	5.7E+04		3.8E+03	1.1E+00	107.1
5.5	1.5E-03	422.0	9.6E+00	1.3E-01	5.6E+04		2.3E+03	1.0E+00	104.4
6.0	1.7E-03	500.0	1.1E+01	1.5E-01	5.6E+04		2.1E+03	1.0E+00	103.9

Table 3. Rectilinear pipe data.

Experimental Data						Moody Chart Data			Statistical Parameters (Values in Module)		
Flow / $m^3 h^{-1}$	Flow / $m^3 s^{-1}$	Head Loss / mmHg	Head Loss / mH_2O	Unit Head Loss / $mH_2O\ m^{-1}$	Friction Factor	Flow Velocity / $m\ s^{-1}$	Reynolds Number	Friction Factor	Absolute Deviate	Relative Deviate	Percentage Deviation/%
3.0	8.3E-04	4.0	5.4E-02	2.5E-02	2.8E-02	8.0E-01	2.9E+04	3.6E-02	8.1E-03	3.5E+00	345.4
4.0	1.1E-03	5.0	6.8E-02	3.1E-02	2.0E-02	1.1E+00	3.9E+04	3.5E-02	1.5E-02	1.3E+00	127.7
5.0	1.4E-03	8.0	1.1E-01	4.9E-02	2.0E-02	1.3E+00	4.8E+04	3.5E-02	1.4E-02	1.4E+00	139.6
6.0	1.7E-03	11.0	1.5E-01	6.8E-02	1.9E-02	1.6E+00	5.8E+04	3.4E-02	1.5E-02	1.3E+00	127.9
7.0	1.9E-03	16.0	2.2E-01	9.9E-02	2.1E-02	1.9E+00	6.8E+04	3.4E-02	1.4E-02	1.5E+00	152.1
8.0	2.2E-03	20.0	2.7E-01	1.2E-01	2.0E-02	2.1E+00	7.8E+04	3.4E-02	1.4E-02	1.4E+00	136.6
9.0	2.5E-03	25.0	3.4E-01	1.5E-01	1.9E-02	2.4E+00	8.7E+04	3.4E-02	1.5E-02	1.3E+00	132.7

Equation 1 was used in the calculations of the algebraic determination of the local head loss coefficients of the fully open ball valve and of the module of forty-four 90º elbows. In the determination of the friction factor value of rectilinear pipe were used the Eqs. 2 and 3, derived from the Darcy-Weisbach equation (Eq. 4). Parallelly, the friction factor also was estimated by Moody's diagram (Fig. 7). For this, it was used the relative roughness value (ε/D) of 0.0071, obtained of cast iron roughness (ε = 0.26)[2] and the Reynolds numbers correspondents to each volumetric flow rate were calculated considering the kinematic viscosity of water of 1.0E-06 $m^2 s^{-1}$, pipe diameter of 0.0365 m, and using Eq. 5. Besides that, statistical parameters – arithmetic mean (M, Eq. 6); absolute deviate (AD, Eq. 7); relative deviate (RD, Eq. 8); percentage deviation (PD, Eq. 9); and mean absolute deviate (MAD, Eq. 10) – were applied to the experimentally obtained data in tests 1, 2, and 3. All results were presented in Tabs. 1, 2, and 3.

$$K_1 = \frac{\Delta H}{Q^2} \quad (1)$$

where: K_1 = constant relative to flow and pressure variation readings [$mH_2O (m^3 s^{-1})^{-2}$]; ΔH_L = head loss variation [mH_2O]; Q = flow [$m^3 s^{-1}$].

$$J = \frac{\Delta H}{L} \quad (2)$$

where: J = unit head loss [$mH_2O\ m^{-1}$]; ΔH = head loss variation [mH_2O]; L = length of pipe [m].

$$f = \frac{J}{\frac{8}{\pi^2 D^5 g} Q^2} \quad (3)$$

where: f = friction factor [unitless]; J = unit head loss [$mH_2O\ m^{-1}$]; D = diameter of pipe [m]; g = gravitational acceleration [9.81 $m^3 s^{-2}$]; Q = flow [$m^3 s^{-1}$].

$$\Delta H = f \frac{L}{D} \frac{V^2}{2g} \quad (4)$$

where: ΔH = head loss variation [mH_2O]; f = friction factor [unitless]; L = length of pipe [m];

Eclética Química Journal, vol. 45, n. 3, 2020, 47-56
ISSN: 1678-4618
DOI: 10.26850/1678-4618eqj.v45.3.2020.p47-56

D = pipe diameter [m]; V = flow velocity [m s^{-1}]; g = gravitational acceleration [9.81 m s^{-2}].

$$Re = \frac{VD}{\nu} \quad (5)$$

where: Re = Reynolds number [unitless]; V = average velocity of flow [m s^{-1}]; D = diameter of pipe [m]; ν = kinematic viscosity of fluid [m^2 s^{-1}].

$$M = \frac{m_1 + m_2 + m_3 + \ldots + m_n}{n} \quad (6)$$

where: M = arithmetic mean; m_1, m_2, m_3, m_n = measures; n = measures number.

$$AD = measure - M \quad (7)$$

where: AD = absolute deviate; M = arithmetic mean.

$$RD = {}^{AD}/_{M} \quad (8)$$

where: RD = relative deviate; AD = absolute deviate; M = arithmetic mean.

$$PD = |\ RD\ x\ 100\ |\% \quad (9)$$

where: PD = percentage deviation; RD relative deviate.

$$MAD = \frac{AD_1 + AD_2 + AD_3 + \ldots + AD_n}{n} \quad (10)$$

where: MAD = mean absolute deviate; AD_1, AD_2, AD_3, AD_n = AD_1, AD_2, AD_3, AD_n = absolute deviates; n = measures number.

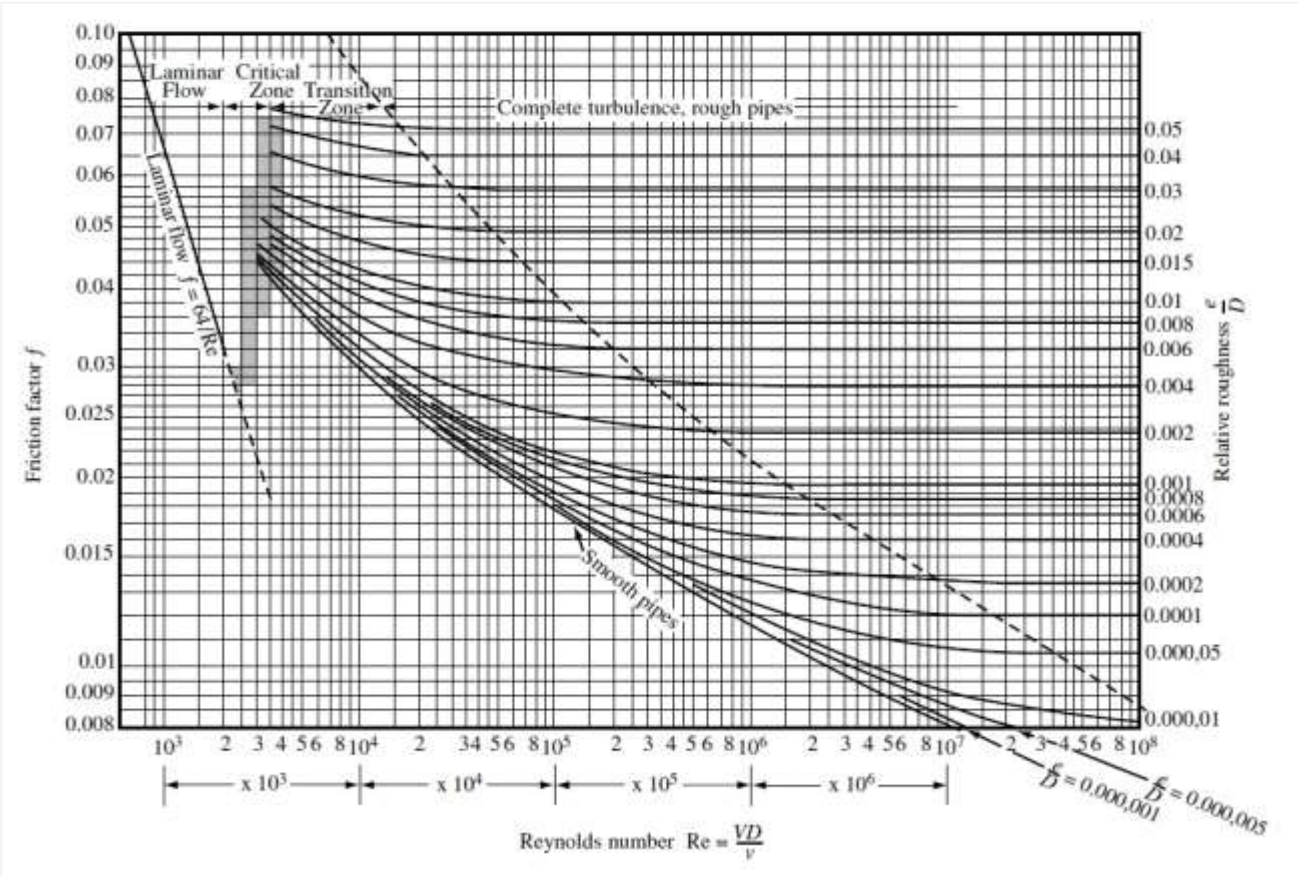

Figure 7. The Moody diagram for the Darcy-Weisbach friction factor.
Source: Larock, Jeppson & Watters[1].

Eclética Química Journal, vol. 45, n. 3, 2020, 47-56
ISSN: 1678-4618
DOI: 10.26850/1678-4618eqj.v45.3.2020.p47-56

3. Results and Discussion

Major and minor head losses were satisfactorily investigated via experimental measurements in the studied hydraulic flow circuit. Figures 8, 9, and 10 exhibit the curves of head loss versus volumetric flow rate for BV-1, 90E-8, and RP-11, respectively. As can be seen, a parabolic profile was presented by both hydraulic circuit's components, corroborating the proportionality relationship between the frictional and minor losses, and the flow velocity, foreseen by the Darcy-Weisbach equation. So, since flow velocity is directly proportional to the volumetric flow rate, the system head loss must be directly proportional to the square of the volumetric flow rate. Table 4 shows the potential regressions fitted to experimental data with its correspondent correlation coefficients (R^2), as well the head loss experimental equations of aforementioned components.

For purposes of determining the head loss coefficients through BV-1 and 90E-8, the localized head loss equation was written as a function of the volumetric flow rate (Eq. 11)[12]. The algebraic determination of the loss coefficients was given by the ratio between the constant relative to measurements of variability in flow rate and the corresponding pressure loss (K_1) and the constant relative to installation data (k_I). Table 5 lists the recorded results for localized head losses coefficients. The attained difference between the theoretical and experimental values was associated with readings' fluctuations, arising from the unstable operating conditions that always occur in closed-loop pump systems due to pressure pulsation. Beyond the fluctuations related to the centrifugal pump's adjusting to each degree of opening of the control valve in the changing the volumetric flow rate of the fluid[12].

$$\Delta H_L = K_L \frac{V^2}{2g} \therefore \overset{V=\frac{4Q}{\pi D^2}}{\therefore} \therefore \Delta H_L = K_L\left(\frac{16}{\pi^2 D^4 2g}\right)Q^2 \therefore \overset{k_I=\left(\frac{8}{\pi^2 D^4 g}\right)Q^2}{\therefore} \therefore \Delta H_L = K_L k_I Q^2 \therefore \Delta H_L = K_1 Q^2 \quad (11)$$

where: ΔH_L = localized head loss variation [mH_2O]; K_L = local head loss coefficient; V = flow velocity [$m\ s^{-1}$]; Q = flow [$m^3\ s^{-1}$]; D = pipe diameter [m]; g = gravitational acceleration [9.81 $m\ s^{-2}$]; k_I = constant relative to installation data; K_1 = constant relative to flow and pressure variation readings.

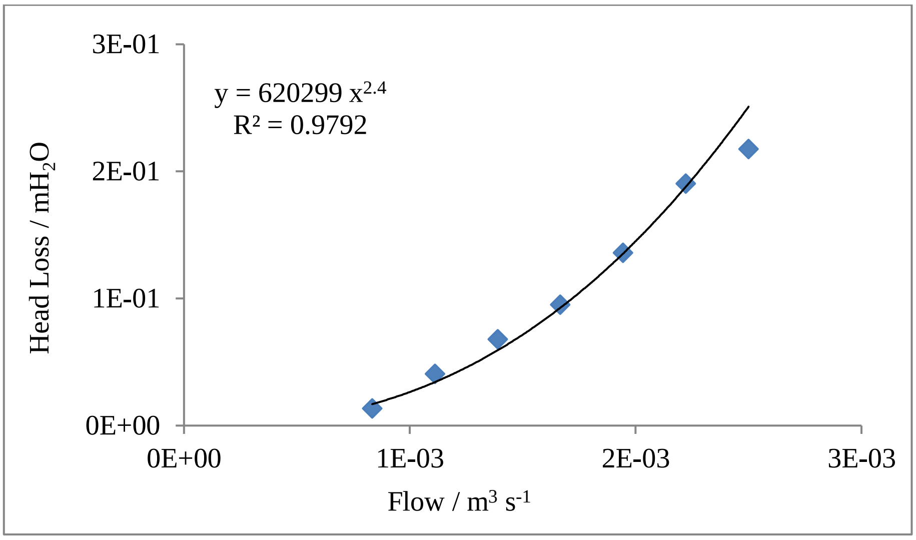

Figure 8. Head loss curve for the ball valve.

Eclética Química Journal, vol. 45, n. 3, 2020, 47-56
ISSN: 1678-4618
DOI: 10.26850/1678-4618eqj.v45.3.2020.p47-56

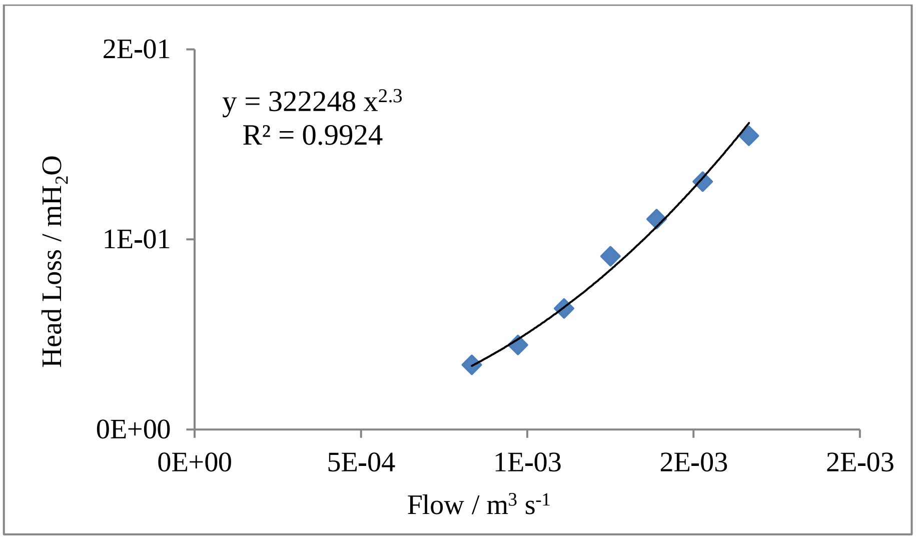

Figure 9. Head loss curve for the 90º elbow.

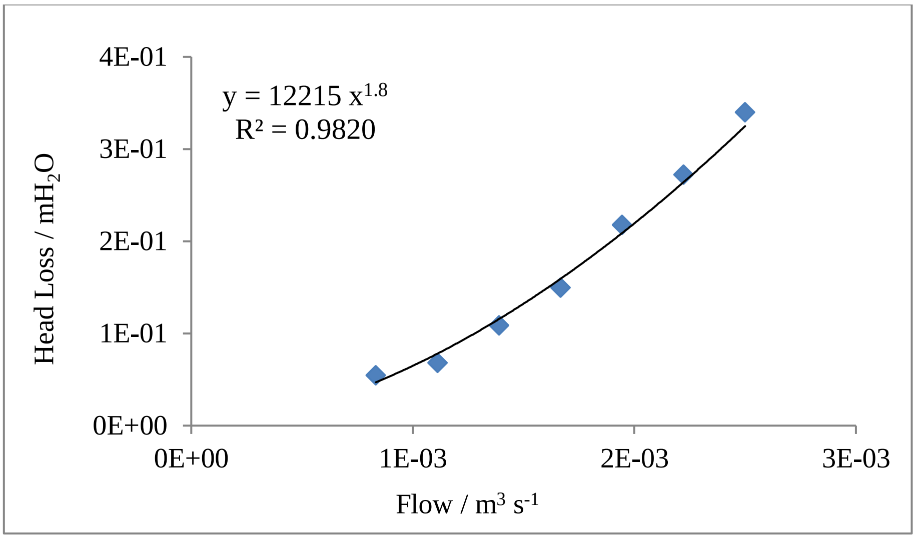

Figure 10. Head loss curve for the rectilinear pipe.

Table 4. Hydraulic circuit components parameters and equations determined from experimental data.

Hydraulic Circuit Component	Head Loss Experimental Equation	Potential Regression	Correlation Coefficient (R^2)
BV-1	$\Delta H = 33000\,Q^2$	$y = 620299\,x^{2.4}$	0.9792
90E-8	$\Delta H = 54000\,Q^2$	$y = 322248\,x^{2.3}$	0.9924
RP-11	–	$y = 12215\,x^{1.8}$	0.9820

Table 5. Constants and coefficients of localized head losses through ball valve and 90º elbows module.

Hydraulic Circuit Component	Experimental Data Constant / $mH_2O\ (m^3\ s^{-1})^{-2}$	Constant Relative to Installation Data	Head Loss Theoretical Coefficient[1]	Head Loss Experimental Coefficient
BV-1	3.3E+04	4.655E+04	7.00E+10	7.10E–01
90E-8	5.4E+04		9.00E–01	1.15E+00

Friction factor value of rectilinear pipe of used cast-iron (RP-11) was satisfactorily determined by the application of the Darcy-Weisbach equation (Eq. 2)[12] to the experimental data. Similarly, the Moody diagram application proved to be a quite appropriate tool to evaluate the effects of relative roughness (0.0071) on a function of Reynolds number (29069 to 87208) in friction factor estimates. The recorded factors via chart were obtained in the turbulent transition zone, in which the Colebrook-White equation (Eq. 12)[12] can be used to replicate numerically the experimental data, located below of region of complete turbulence for rough pipes and above of region of smooth turbulence. By comparing the factors obtained via experimental measurements and via diagram, a good approximation between the values was observed, with mean absolute deviation of 0.0136.

$$\frac{1}{\sqrt{f}} = 1.14 - \left(2\, log_{10} \frac{\varepsilon}{D}\right) + \left(\frac{9.35}{Re\sqrt{f}}\right) \qquad (12)$$

where: f = friction factor [unitless]; ε = pipe roughness [mm]; D = pipe diameter [mm]; Re = Reynolds number [unitless].

Fluid mechanic's fundamentals to the internal turbulent flow of water as fluid flow in a hydraulic circuit were rightly applied. Normal head losses produced by fluid viscous effects and the localized losses depending on the geometry singularities of the pipe were successfully determined. Viscous effects on flow and head losses associated with the piping design were discussed. Characteristics such as the pipe roughness, as well as velocity and viscosity of the fluid were used as parameters for algebraic determination of the friction factor value associated with the circuit's rectilinear pipe. Experimental coefficients of localized losses through ball valve and 90º elbows module were measured and compared with its respective theoretical values.

This work showed how simple measures of volumetric flow rate and the pressure variation may be useful to measure major and minor head losses in hydraulic drainage networks and how Moody's diagram can be applied to understand the behavior of viscous flows and evaluate the loss of energy due to viscous friction. Furthermore, the results provided could be useful to solve flow problems in surcharged hydraulic systems where the head losses cannot be neglected or for dimensioning and optimization studies of design parameters of drainage networks of groundwater flow and hydraulic transport. So, hydraulic calculations estimates can help avoid several problems, such as inappropriate drainage pipes, insufficient carrying capacities, and the occurrence of floods, already that the theory alone is unable entirely to quantify the magnitudes of the energy hydraulic losses.

4. Conclusions

Measurements of variability in volumetric flow rate and the corresponding pressure loss, as well Moody's diagram application allowed to investigate major and minor head losses associated water flow in the studied hydraulic circuit, suggesting the suitability of the proposed methodology. Experimental data generated curves of head loss and their well fitted to potential regressions, displaying correlation coefficients (R^2) of 0.9792, 0.9924, and 0.9820 for ball valve, 90º elbows module, and rectilinear pipe, respectively. Head loss experimental equations and local loss coefficients through ball valve and 90º elbows module were determined successfully. The Moody's diagram application proved to be a quite appropriate tool for an approximate estimation and with reasonable accuracy of friction factor value of rectilinear pipe of used cast-iron. A good approximation between factors values obtained via experimental measurements and the diagram was observed with mean absolute deviate of 0.0136.

5. References

[1] Larock, B. E., Jeppson, R. W., Watters, G. Z., Hydraulics of pipeline systems, CRC Press LLC, Boca Raton, 2000.

[2] Jo, J. B., Kim, J. S., Yoon, S. E., Experimental estimation of the head loss coefficient at surcharged four-way junction manholes, Urban Water Journal 15 (8) (2018) 780-789. https://doi.org/10.1080/1573062X.2018.1547408.

[3] Colebrook, C. F., Turbulent flow in pipes, with particular reference to the transition region between the smooth and rough pipe laws, Journal of the Institution

Eclética Química Journal, vol. 45, n. 3, 2020, 47-56
ISSN: 1678-4618
DOI: 10.26850/1678-4618eqj.v45.3.2020.p47-56

of Civil Engineers 11 (4) (1939) 133-156. http://doi.org/10.1680/ijoti.1939.13150.

[4] Moody, L. F., Princeton, N. J., Friction factors for pipe flow, Transactions of the American Society of Mechanical Engineers 66 (1944) 671-681.

[5] Chen, Z., Qian, J-Z., Luo, S-H., Zhan, H-B., Experimental study of friction factor for groundwater flow in a single rough fracture, Journal of Hydrodynamics 21 (6) (2009) 820-825. https://doi.org/10.1016/S1001-6058(08)60218-8.

[6] Zeghadnia, L., Robert, J. L., Achour, B., Explicit solutions for turbulent flow friction factor: A review, assessment and approaches classification, Ain Shams Engineering Journal 10 (1) (2019) 243-252. https://doi.org/10.1016/j.asej.2018.10.007.

[7] Brkić, D., Ćojbašić, Ž., Evolutionary optimization of colebrook's turbulent flow friction approximations, Fluids 2 (2) (2017) 15. https://doi.org/10.3390/fluids2020015.

[8] LaViolette, M., On the history, science, and technology included in the moody diagram, Journal of Fluids Engineering 139 (3) (2017) 030801. https://doi.org/10.1115/1.4035116.

[9] Graham, L. J. W., Pullum, L., Wu, J., Flow of non-Newtonian fluids in pipes with large roughness, The Canadian Journal of Chemical Engineering 94 (6) (2016) 1102-1107. https://doi.org/10.1002/cjce.22494.

[10] Dobrnjac, M., Determination of friction coefficient in transition flow region for waterworks and pipelines calculation, Annals of the Faculty of Engineering Hunedoara 10 (3) (2012) 137-142. http://annals.fih.upt.ro/pdf-full/2012/ANNALS-2012-3-21.pdf.

[11] Ulusarslan, D., Effect of diameter ratio on loss coefficient of elbows in the flow of low-density spherical capsule trains, Particulate Science and Technology 28 (4) (2010) 348-359. https://doi.org/10.1080/02726351003702558.

[12] Buonicontro, C. M. S., Laboratório de fluidomecânicos: práticas de máquinas de fluxo, PUC Minas, Belo Horizonte, 2010. https://pt.scribd.com/document/56230307/Manual-Laboratorio-MaqFluxo-1%C2%BA2010A.

Eclética Química Journal, vol. 45, n. 3, 2020, 47-56
ISSN: 1678-4618
DOI: 10.26850/1678-4618eqj.v45.3.2020.p47-56